JACS
JOURNAL OF THE AMERICAN CHEMICAL SOCIETY
pubs.acs.org/JACS
Communication

Reaction Discovery Using Spectroscopic Insights from an Enzymatic C−H Amination Intermediate

Anuvab Das,[‡] Shilong Gao,[‡] Ravi G. Lal, Madeline H. Hicks, Paul H. Oyala, and Frances H. Arnold*

Cite This: J. Am. Chem. Soc. 2024, 146, 20556−20562
Read Online
ACCESS | Metrics & More | Article Recommendations | Supporting Information

ABSTRACT: Engineered hemoproteins can selectively incorporate nitrogen from nitrene precursors like hydroxylamine, *O*-substituted hydroxylamines, and organic azides into organic molecules. Although iron-nitrenoids are often invoked as the reactive intermediates in these reactions, their innate reactivity and transient nature have made their characterization challenging. Here we characterize an iron-nitrosyl intermediate generated from NH_2OH within a protoglobin active site that can undergo nitrogen-group transfer catalysis, using UV−vis, electron paramagnetic resonance (EPR) spectroscopy, and high-resolution electrospray ionization mass spectrometry (HR-ESI-MS) techniques. The mechanistic insights gained led to the discovery of aminating reagents—nitrite (NO_2^-), nitric oxide (NO), and nitroxyl (HNO)—that are new to both nature and synthetic chemistry. Based on the findings, we propose a catalytic cycle for C−H amination inspired by the nitrite reductase pathway. This study highlights the potential of engineered hemoproteins to access natural nitrogen sources for sustainable chemical synthesis and offers a new perspective on the use of biological nitrogen cycle intermediates in biocatalysis.

Nitrogen is crucial for all life forms on Earth due to its widespread presence in biomolecules and natural products.[1−3] Moreover, nitrogen-containing compounds are essential in the pharmaceutical, petrochemical, and agrochemical industries.[4−7] Atmospheric nitrogen (N_2), which accounts for 78% of the Earth's atmosphere, serves as the primary source for all nitrogen-containing compounds in nature. N_2 cannot be directly assimilated, however, and must first be converted into ammonia (NH_3) through nitrogen fixation, and afterward undergoes various transformations within the nitrogen cycle to become accessible to living organisms (Figure 1a).[2,8−13] Despite the variety of potential nitrogen sources produced through the nitrogen cycle, natural enzymes are not known to use those for C−H bond amination. Instead, biological systems rely on prefunctionalized carbon centers to introduce nitrogen functionality, typically by employing enzymatic processes such as reductive amination, transamination, or hydroamination.[14]

Inspired by Dawson and Breslow's demonstration that a cytochrome P450 can catalyze C−H amination via a putative iron-nitrenoid intermediate,[15] researchers many years later developed biocatalytic nitrene transfer for selective construction of C−N bonds.[16,17] In particular, iron-nitrenoids have emerged as powerful intermediates for C−H amination and olefin aziridination using these engineered enzymes.[18−23] Previous reports have shown that hemoproteins can activate organic azides and *O*-substituted hydroxylamines, forming and transferring nitrenes to hydrocarbons (Figure 1b).[16,24−30] Although these synthetic reagents are effective in generating an array of C−N bonds, they also produce significant amounts of byproducts and present sustainability challenges.

We are interested in engineering enzymes that can utilize natural nitrogen sources for amination. Such engineered reactivity might point to naturally occurring C−H functionalizing "nitrene transferases", akin to the discovery that cytochrome P450BezE is a naturally occurring olefin functionalizing nitrene transferase that processes an *O*-acetylated hydroxylamine precursor.[31] The discovery and development of new amination reactions would benefit from mechanistic understanding of the intermediates involved. However, the exceptional reactivity of iron-nitrenoid species, which makes them attractive for catalysis, also renders them challenging to characterize.[32−38] Thus, efforts to develop new and sustainable reactions mostly relies on insights from computational methods.[39−41]

Recently, we engineered a protoglobin from *Pyrobaculum arsenaticum* to catalyze amination of benzylic C−H bonds using hydroxylamine (NH_2OH) as the aminating reagent.[42] NH_2OH plays a crucial role as an intermediate in the nitrogen cycle, and the enzymatic reaction produces water as the sole byproduct. We proposed formation of an iron-nitrenoid intermediate from NH_2OH analogous to generating Compound I from the hydroperoxo intermediate in the peroxygenase catalytic cycle, given that NH_2OH is structurally and electronically analogous to hydrogen peroxide (H_2O_2).[43,44] However, in contrast to the peroxygenase cycle, the NH_2OH-mediated aminase cycle operates under a reducing environment. The exact mechanism by which NH_2OH promotes amination is unknown. To obtain a better mechanistic understanding, we investigated the nitrogen-group

Received: April 26, 2024
Revised: July 11, 2024
Accepted: July 15, 2024
Published: July 22, 2024

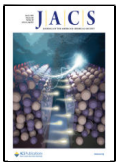

https://doi.org/10.1021/jacs.4c05761
J. Am. Chem. Soc. 2024, 146, 20556−20562

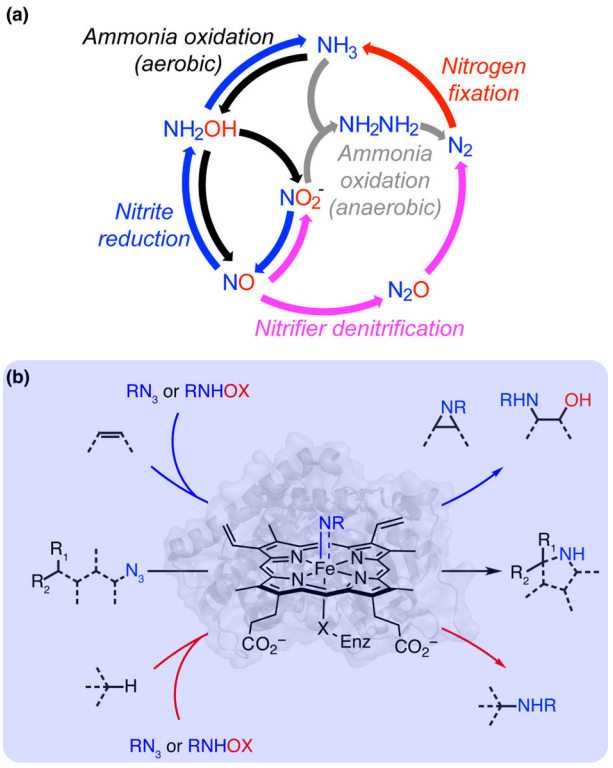

Figure 1. (a) Simplified depiction of the biological nitrogen cycle, highlighting the nitrogen intermediates that could be leveraged to develop new amination reactions. (b) Previous biocatalytic nitrene transfer reactions used chemically synthesized organic azides and *O*-substituted hydroxylamines as nitrogen precursors.

transfer chemistry by protoglobin using NH_2OH, employing spectroscopic techniques for our analysis. Moreover, considering the role of NH_2OH in the nitrogen cycle, we hypothesized that investigating the mechanism could give insights into how to access other naturally occurring nitrogen intermediates.

We initiated these studies by examining the spectral features of protoglobin variant ParPgb-HYA-5213, engineered to activate NH_2OH, under different redox conditions (Figure 2a). UV−vis analysis of the resting state of ParPgb-HYA-5213 ($\boldsymbol{E}_{ox}$) in solution shows a Soret band at 413 nm and a broad Q-band at 543 nm. The addition of a 200-fold excess of sodium dithionite ($Na_2S_2O_4$) relative to $\boldsymbol{E}_{ox}$ results in the reduced form of the protein, $\mathbf{E}_{red}$, and shifts the bands to 434 and 562 nm. Meanwhile adding a 600-fold excess of NH_2OH relative to $\mathbf{E}_{red}$ instantaneously generates a new spectrum with bands at 425, 530, and 560 nm. In contrast, addition of NH_2OH to $\boldsymbol{E}_{ox}$ does not alter the spectrum (Figure S1), suggesting that NH_2OH interacts with $\mathbf{E}_{red}$ to form $\mathbf{E}_{redHA}$.

Interestingly, $\mathbf{E}_{redHA}$ is not indefinitely stable and decomposes under ambient conditions through well-defined isosbestic points at 438 and 572 nm (Figure 2b). The presence of distinct isosbestic points indicates the absence of a steady-state intermediate. UV−vis analysis of the reaction mixture indicates the evolution of $\boldsymbol{E}_{ox}$ (Figure S2). In the presence of a benzylic C−H-containing substrate, the conversion of $\mathbf{E}_{redHA}$ to $\boldsymbol{E}_{ox}$, occurs more rapidly (Figure S3) and is accompanied by the formation of aminated product, as determined by HPLC-MS.

To obtain further information regarding the reactive intermediate involved in amination, we carried out electron paramagnetic resonance (EPR) experiments. X-band CW-EPR spectra of $\boldsymbol{E}_{ox}$, $\mathbf{E}_{red}$, and $\mathbf{E}_{redHA}$ display no $S = 1/2$ signals at 77

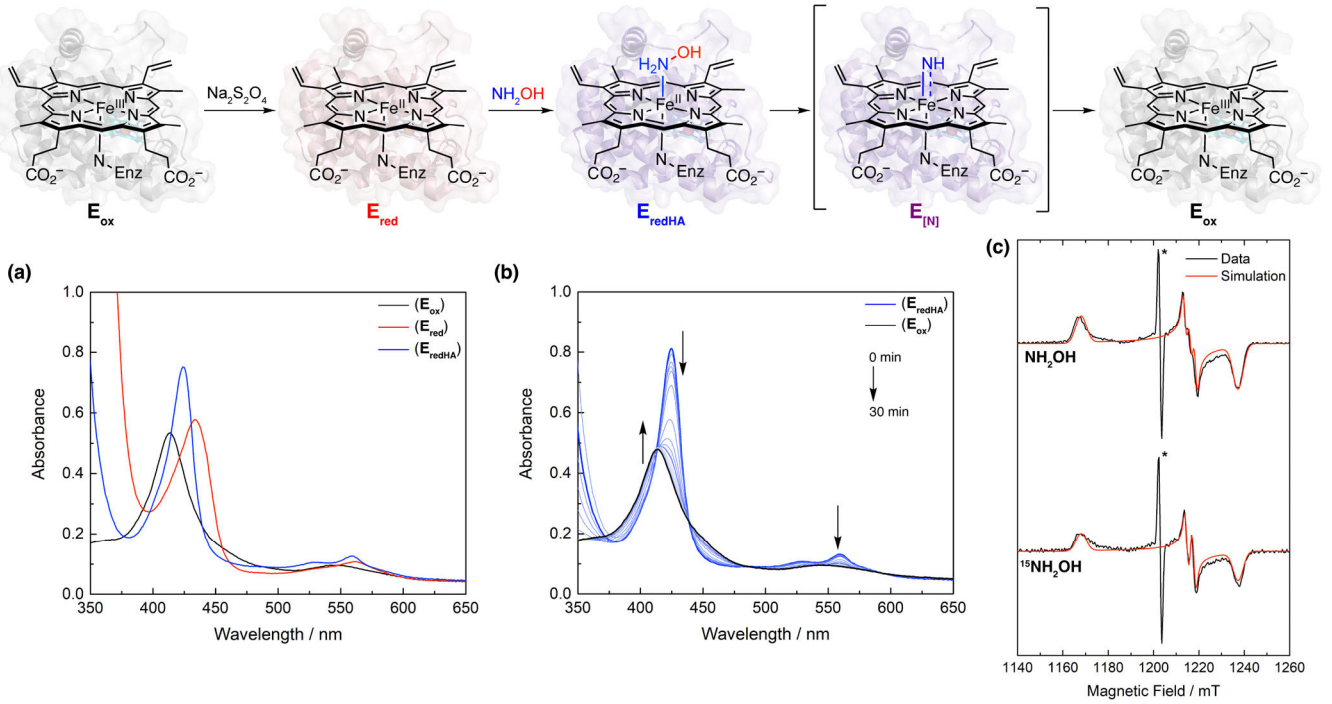

Figure 2. (a) UV−vis spectra of ParPgb-HYA-5213 protein in its resting state ($\boldsymbol{E}_{ox}$) and its reduced state ($\mathbf{E}_{red}$) and the hydroxylamine adduct of the reduced protein ($\mathbf{E}_{redHA}$). (b) UV−vis spectra collected during the decomposition of $\mathbf{E}_{redHA}$ to $\boldsymbol{E}_{ox}$, with isosbestic points at 438 and 572 nm. (c) Experimental (black line) and simulated (red line) Q-band pseudomodulated EPR spectra of the EPR-active species in a frozen solution at 15 K, obtained by mixing $\mathbf{E}_{red}$ with NH_2OH or $^{15}NH_2OH$. *Indicates a signal arising from the resonator background. See the SI for experimental details and simulation parameters.

https://doi.org/10.1021/jacs.4c05761
J. Am. Chem. Soc. 2024, 146, 20556−20562

K (Figure S4), indicating that the heme exists in a high-spin configuration. However, the addition of 600-fold excess of NH_2OH relative to $\mathbf{E_{red}}$ produces a rhombic EPR signal at 77 K with *g*-values near $g = 2$ ($g = [2.087, 2.004, 1.970]$), consistent with a ground spin-state of $S = 1/2$ (Figure S4). Comparison of the EPR signal with that of free hemin, along with varying concentrations of protein and heme loading, revealed that the signal is dependent on heme-bound protein (Figures S5 and S6). Additionally, mutating the axial ligand from histidine to methionine alters the redox potential of the protein and the *g*-values of the EPR signal (Figures S7 and S8).[45]

Next, we investigated the stability of the EPR-active species by monitoring its signal intensity over time. The EPR signal appears instantly upon addition of NH_2OH at $t = 0$, reaching a maximum at $t = 5$ min. The signal intensity then starts to decay and completely disappears by $t = 30$ min (Figure S9). Moreover, to confirm that the signal depends on NH_2OH, we compared the hyperfine coupling of the EPR signal using both naturally abundant and ^{15}N-labeled hydroxylamine. Differences between these isotopologues in the X-band CW-EPR spectra (Figure S10) were only clearly discernible at the intermediate *g*-value ($g \approx 2.004$), and only well-resolved at temperatures lower than 77 K (Figure S11), perhaps owing to T_1 broadening or involvement of thermally accessible excited states at higher temperatures. To probe the electronic structure of this intermediate, we turned to higher frequency Q-band (34 GHz) pulse EPR spectroscopy. We observe a very distinct difference in the hyperfine splitting at the intermediate *g*-value in ^{15}N-labeled samples (Figure 2c and Table S1). This change in the hyperfine coupling pattern confirms the electron spin interacting with NH_2OH.

We hypothesized that the nitrogen incorporation reactivity arises from the nitrenoid radical species, $\mathbf{E_{[N]}}$. However, $\mathbf{E_{[N]}}$ would not exhibit an $S = 1/2$ EPR signal; hence, we examined the reaction using the spin-trap 5,5-dimethylpyrroline-*N*-oxide (DMPO, **1**).[46−48] Compound **1** is EPR-silent; however, the reaction mixture — prepared by adding an excess of NH_2OH to $\mathbf{E_{red}}$, followed by the addition of an excess of **1** after 5 min — becomes EPR-active. The DMPO adducts generated from either NH_2OH or $^{15}NH_2OH$ are sufficiently stable for observation by room temperature X-band CW-EPR (Figure 3a and Table S2). High-resolution electrospray ionization mass spectrometry (HR-ESI-MS) of the spin-trapped sample of NH_2OH shows a mass at $m/z = 129.1024$, corresponding to the DMPO-adduct (**2-NH$_2$**), while the HR-ESI-MS of the spin-trapped EPR sample of $^{15}NH_2OH$ displays a mass at $m/z = 130.0999$, corresponding to the DMPO-adduct (**2-^{15}NH$_2$**) (Figure 3b). The spin-trapped EPR data and the corresponding HR-ESI-MS results strongly suggest that the reaction proceeds through a nitrenoid radical species.[33,47]

During our investigation into the EPR-active species, we discovered that the features of the EPR spectra were similar to those of a six-coordinate iron-nitrosyl $\{FeNO\}^7$ species.[12,13,49−59] This prompted us to look for enzymatic pathways involving hemoproteins while also containing NH_2OH and NO as intermediates. We identified two: aerobic ammonia oxidation and the nitrite reductase pathways.[57−63] The similarity between engineered protoglobin-mediated nitrogen incorporation and the nitrite reductase pathway led us to investigate the intermediates of this pathway as potential aminating reagents (Figure S12).[64−66]

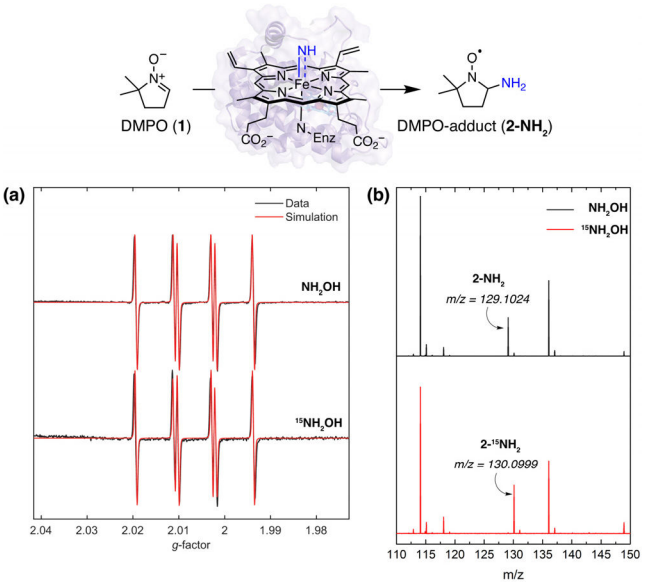

Figure 3. (a) Experimental (black line) and simulated (red line) X-band CW-EPR spectra of the DMPO adducts, obtained by mixing $\mathbf{E_{red}}$ and **1** in solution at room temperature with NH_2OH or $^{15}NH_2OH$. (b) HR-ESI-MS spectra of the DMPO adducts obtained by treating $\mathbf{E_{red}}$ and **1** with NH_2OH or $^{15}NH_2OH$.

To investigate the potential of nitrogen cycle intermediates to serve as aminating reagents, we first analyzed the UV−vis spectral features of $\mathbf{E_{red}}$ in the presence of an excess of NO_2^-, NO, and HNO (Figures S13−S15). The reaction mixtures with NO_2^- and NO displayed spectral features at 422 and 568 nm, which gradually decayed over 100 min, resulting in the formation of $\boldsymbol{E_{ox}}$. Conversely, the mixture with HNO exhibited spectral features like those with NH_2OH and decayed to $\boldsymbol{E_{ox}}$ over 30 min. Thus, the formation of $\boldsymbol{E_{ox}}$ is slower with NO_2^- and NO than with HNO and NH_2OH.

Next, we investigated the EPR features of $\mathbf{E_{red}}$ by exposing it to an excess of NO_2^-, NO, HNO, and $^{15}NO_2^-$, analyzing the results using both X-band CW-EPR (Figure S11) and Q-band pulse field-swept EPR spectra (Figure 4a and Table S1). Furthermore, the HR-ESI-MS analysis of the DMPO spin-trapped sample with $\mathbf{E_{red}}$ and NO_2^- revealed a mass at $m/z = 129.1021$, corresponding to **2-NH$_2$** (Figure 4b and 4c). These results indicate that the activation of NH_2OH, NO_2^-, NO, and HNO by $\mathbf{E_{red}}$ leads to the formation of a common iron-nitrosyl intermediate that can further generate an iron-nitrenoid intermediate downstream (Figures S16−S29 and Table S3).[67−70]

Since ParPgb-HYA-5213 effectively aminates *p*-ethylanisole (**3**) with NH_2OH, we explored its activity with the other nitrogen reagents. We found that all of them can promote benzylic C−H amination of **3**, yielding **4-NH$_2$** (Figure 4b and 4d). Specifically, NH_2OH achieves a yield of 90.7% with >99% enantiomeric excess (*ee*), NO_2^- results in 26.2% yield and >99% *ee*, NO provides 17.8% yield and >99% *ee*, and HNO yields 89.8% with >99% *ee* (Figure 4d and SI Sections 1.3 and 1.4). Furthermore, $^{15}NH_2OH$ and $^{15}NO_2^-$ also give **4-^{15}NH$_2$** with moderate-to-high yield and excellent enantioselectivity. The nitrogen incorporation reactivity suggests that the iron-nitrosyl species is an on-pathway intermediate (Figure S30), and the high enantioselectivity indicates that the reaction occurs within the enzyme active site.

https://doi.org/10.1021/jacs.4c05761
J. Am. Chem. Soc. 2024, 146, 20556−20562

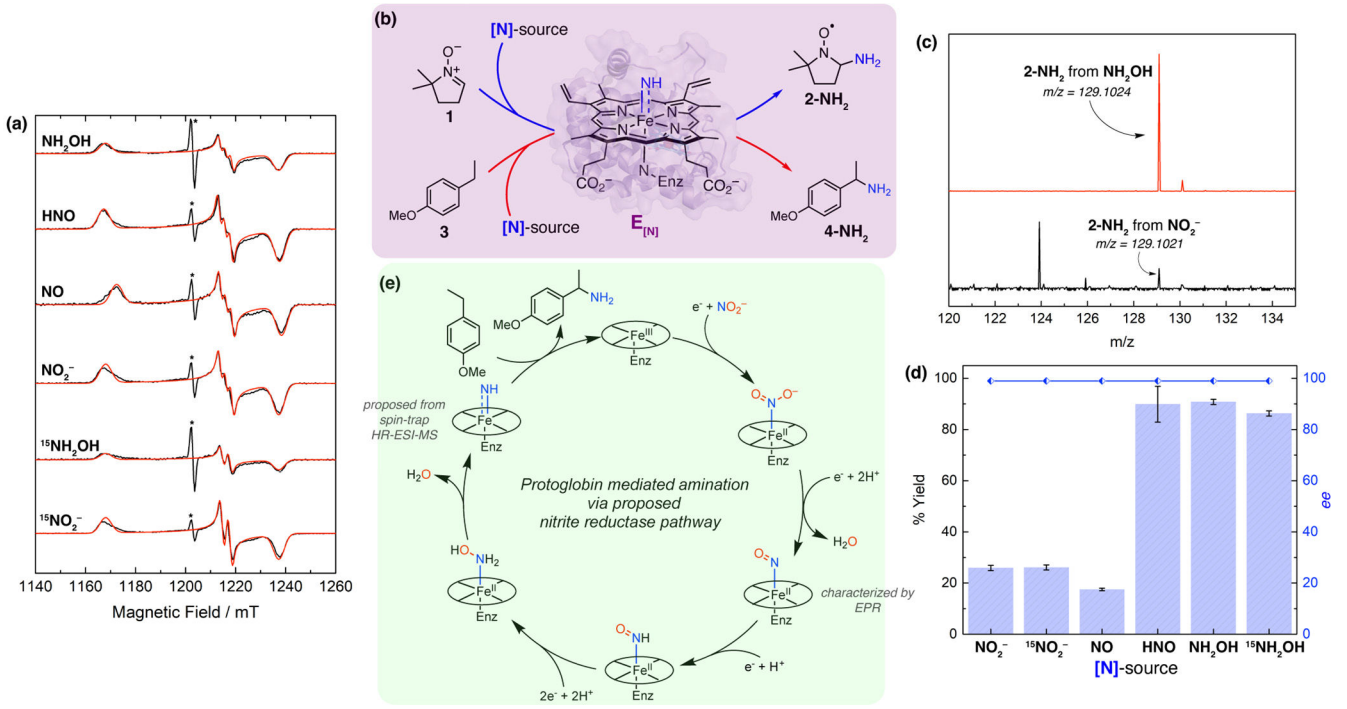

Figure 4. (a) Experimental (black line) and simulated (red line) Q-band pseudomodulated EPR spectra of the putative {FeNO}^{7} species in a frozen solution at 15 K, obtained by mixing $\mathbf{E_{red}}$ with different aminating reagents such as NH_2OH, NO_2^-, NO, HNO, $^{15}NH_2OH$, or $^{15}NO_2^-$. *Indicates a background signal from the resonator. (b) The reduced ParPgb-HYA-5213 ($\mathbf{E_{red}}$) protein, when treated with NH_2OH or NO_2^-, transfers the nitrogen group to form **2-NH$_2$** and **4-NH$_2$** from **1** and **3**, respectively. (c) HR-ESI-MS spectrum of the DMPO adducts, obtained by treating $\mathbf{E_{red}}$ and **1** with NH_2OH or NO_2^-. (d) Biocatalytic nitrene transfer to the benzylic C−H bond of **3** to form **4-NH$_2$** with different aminating sources. See the SI for experimental details and optimized reaction conditions. (e) Evidence from the EPR, HR-ESI-MS of spin-trap, and amination product yield and enantioselectivity suggests that protoglobin-mediated benzylic C−H amination goes through a nitrite reductase-type pathway.

Although the protein was originally engineered for nitrogen incorporation using NH_2OH, mechanistic insights revealed its ability to also activate NO_2^-, NO and HNO for nitrogen incorporation. Based on these findings, we propose a new catalytic cycle for protoglobin-mediated C−H amination, inspired by the nitrite reductase pathway (Figure 4e), wherein NO_2^- is reduced by dithionite to NO, then to HNO, then NH_2OH, which finally incorporates nitrogen into organic molecules via a putative iron-nitrenoid intermediate.[70,71] This proposed mechanism also correlates to the lower yields and the slower rate of consumption of NO_2^-, due to the successive reduction steps. However, directed evolution could be used to generate variants that can efficiently activate these new reagents.

In conclusion, we have spectroscopically characterized an iron-nitrosyl intermediate derived from NH_2OH within a protoglobin active site, which we propose generates an iron-nitrenoid intermediate downstream. The mechanistic insights gained from characterizing the iron-nitrosyl intermediate led to the discovery of NO_2^-, NO, and HNO as nitrene precursors for C−H amination. Based on the evidence from EPR, HR-ESI-MS, and amination product yield and enantioselectivity, we have proposed a catalytic cycle for C−H amination using these reagents inspired by the nitrite reductase pathway. This study highlights the potential of engineered hemoproteins to access natural nitrogen sources for sustainable chemical synthesis, offering a new perspective on the utilization of nitrogen cycle intermediates in biocatalysis. These insights could pave the way for further exploration of natural metabolic pathways and might lead to the discovery of naturally occurring C−H functionalizing "nitrene transferases".

■ ASSOCIATED CONTENT

Supporting Information

The Supporting Information is available free of charge at https://pubs.acs.org/doi/10.1021/jacs.4c05761.

Materials, experimental methods, and additional characterization data including Figures S1−S30 and Tables S1−S3 (PDF)

■ AUTHOR INFORMATION

Corresponding Author

Frances H. Arnold − *Division of Chemistry and Chemical Engineering, California Institute of Technology, Pasadena, California 91125, United States;* orcid.org/0000-0002-4027-364X; Email: frances@cheme.caltech.edu

Authors

Anuvab Das − *Division of Chemistry and Chemical Engineering, California Institute of Technology, Pasadena, California 91125, United States;* orcid.org/0000-0002-9344-4414

Shilong Gao − *Division of Chemistry and Chemical Engineering, California Institute of Technology, Pasadena, California 91125, United States;* Present Address: Moderna, Boston, Massachusetts 02135, United States; orcid.org/0000-0003-2808-6283

Ravi G. Lal − *Division of Chemistry and Chemical Engineering, California Institute of Technology, Pasadena, California 91125, United States*

Madeline H. Hicks − *Division of Chemistry and Chemical Engineering, California Institute of Technology, Pasadena, California 91125, United States*

Paul H. Oyala − *Division of Chemistry and Chemical Engineering, California Institute of Technology, Pasadena, California 91125, United States;* orcid.org/0000-0002-8761-4667

Complete contact information is available at: https://pubs.acs.org/10.1021/jacs.4c05761

Author Contributions

‡A.D. and S.G. contributed equally.

Funding

This work was supported by the U.S. Department of Energy, Office of Science, Office of Basic Sciences (DE-SC0021141) and the G. Harold & Leila Y. Mathers Foundation (MF-2111-02065) to F.H.A.

Notes

The authors declare no competing financial interest.

This report was prepared as an account of work sponsored by an agency of the United States Government. Neither the United States Government nor any agency thereof, nor any of their employees, makes any warranty, express or implied, or assumes any legal liability or responsibility for the accuracy, completeness, or usefulness of any information, apparatus, product, or process disclosed, or represents that its use would not infringe privately owned rights. Reference herein to any specific commercial product, process, or service by trade name, trademark, manufacturer, or otherwise does not necessarily constitute or imply its endorsement, recommendation, or favoring by the United States Government or any agency thereof. The views and opinions of authors expressed herein do not necessarily state or reflect those of the United States Government or any agency thereof.

■ ACKNOWLEDGMENTS

The authors thank Dr. Nathan Dalleska for assistance with acquiring HR-ESI-MS data using instrumentation at the Resnick Sustainability Institute's Water and Environment Lab at Caltech. The authors thank Dr. Mona Shahgholi for assistance with acquiring LCMS data using instrumentation at the Caltech CCE Multiuser Mass Spectrometry Laboratory. The authors also thank the Dow Next Generation Educator Fund and the Beckman Institute at Caltech for supporting the Caltech EPR facility. The authors also thank Prof. Harry B. Gray, Prof. Jonas C. Peters, Dr. Sabine Brinkmann-Chen and Dr. Edwin Alfonzo for helpful discussions and comments on the manuscript.

■ REFERENCES

(1) Canfield, D. E.; Glazer, A. N.; Falkowski, P. G. The Evolution and Future of Earth's Nitrogen Cycle. *Science* **2010**, *330*, 192−196.

(2) Lehnert, N.; Dong, H. T.; Harland, J. B.; Hunt, A. P.; White, C. J. Reversing nitrogen fixation. *Nat. Rev. Chem.* **2018**, *2*, 278−289.

(3) Galloway, J. N.; Townsend, A. R.; Erisman, J. W.; Bekunda, M.; Cai, Z.; Freney, J. R.; Martinelli, L. A.; Seitzinger, S. P.; Sutton, M. A. Transformation of the Nitrogen Cycle: Recent Trends, Questions, and Potential Solutions. *Science* **2008**, *320*, 889−892.

(4) Vitaku, E.; Smith, D. T.; Njardarson, J. T. Analysis of the Structural Diversity, Substitution Patterns, and Frequency of Nitrogen Heterocycles among U.S. FDA Approved Pharmaceuticals. *J. Med. Chem.* **2014**, *57*, 10257−10274.

(5) Anas, M.; Liao, F.; Verma, K. K.; Sarwar, M. A.; Mahmood, A.; Chen, Z.-L.; Li, Q.; Zeng, X.-P.; Liu, Y.; Li, Y.-R. Fate of nitrogen in agriculture and environment: agronomic, eco-physiological and molecular approaches to improve nitrogen use efficiency. *Biol. Res.* **2020**, *53*, 47.

(6) Pan, S.-Y.; He, K.-H.; Lin, K.-T.; Fan, C.; Chang, C.-T. Addressing nitrogenous gases from croplands toward low-emission agriculture. *npj Clim. Atmos. Sci.* **2022**, *5*, 43.

(7) Banerjee, A.; Armstrong, O.; Girard-Lauriault, P.-L. Synthesis of Higher-Order Nitrogen-Containing Organic Compounds from Butylamine Using a Microsecond Pulse Dielectric Barrier Discharge. *Ind. Eng. Chem. Res.* **2023**, *62*, 14144−14150.

(8) Soler-Jofra, A.; Pérez, J.; van Loosdrecht, M. C. M. Hydroxylamine and the nitrogen cycle: A review. *Water Res.* **2021**, *190*, 116723.

(9) Schalk, J.; de Vries, S.; Kuenen, J. G.; Jetten, M. S. M. Involvement of a Novel Hydroxylamine Oxidoreductase in Anaerobic Ammonium Oxidation. *Biochemistry* **2000**, *39*, 5405−5412.

(10) Caranto, J. D. The emergence of nitric oxide in the biosynthesis of bacterial natural products. *Curr. Opin. Chem. Biol.* **2019**, *49*, 130−138.

(11) Oliveira, C.; Benfeito, S.; Fernandes, C.; Cagide, F.; Silva, T.; Borges, F. NO and HNO donors, nitrones, and nitroxides: Past, present, and future. *Med. Res. Rev.* **2018**, *38*, 1159−1187.

(12) Ferousi, C.; Majer, S. H.; DiMucci, I. M.; Lancaster, K. M. Biological and Bioinspired Inorganic N−N Bond-Forming Reactions. *Chem. Rev.* **2020**, *120*, 5252−5307.

(13) Lehnert, N.; Kim, E.; Dong, H. T.; Harland, J. B.; Hunt, A. P.; Manickas, E. C.; Oakley, K. M.; Pham, J.; Reed, G. C.; Alfaro, V. S. The Biologically Relevant Coordination Chemistry of Iron and Nitric Oxide: Electronic Structure and Reactivity. *Chem. Rev.* **2021**, *121*, 14682−14905.

(14) Alfonzo, E.; Das, A.; Arnold, F. H. New additions to the arsenal of biocatalysts for noncanonical amino acid synthesis. *Curr. Opin. Green Sustain. Chem.* **2022**, *38*, 100701.

(15) Svastits, E. W.; Dawson, J. H.; Breslow, R.; Gellman, S. H. Functionalized nitrogen atom transfer catalyzed by cytochrome P-450. *J. Am. Chem. Soc.* **1985**, *107*, 6427−6428.

(16) Singh, R.; Bordeaux, M.; Fasan, R. P450-Catalyzed Intramolecular sp^3 C−H Amination with Arylsulfonyl Azide Substrates. *ACS Catal.* **2014**, *4*, 546−552.

(17) McIntosh, J. A.; Coelho, P. S.; Farwell, C. C.; Wang, Z. J.; Lewis, J. C.; Brown, T. R.; Arnold, F. H. Enantioselective Intramolecular C−H Amination Catalyzed by Engineered Cytochrome P450 Enzymes In Vitro and In Vivo. *Angew. Chem., Int. Ed.* **2013**, *52*, 9309−9312.

(18) Hyster, T. K.; Farwell, C. C.; Buller, A. R.; McIntosh, J. A.; Arnold, F. H. Enzyme-Controlled Nitrogen-Atom Transfer Enables Regiodivergent C−H Amination. *J. Am. Chem. Soc.* **2014**, *136*, 15505−15508.

(19) Farwell, C. C.; Zhang, R. K.; McIntosh, J. A.; Hyster, T. K.; Arnold, F. H. Enantioselective Enzyme-Catalyzed Aziridination Enabled by Active-Site Evolution of a Cytochrome P450. *ACS Cent. Sci.* **2015**, *1*, 89−93.

(20) Dunham, N. P.; Arnold, F. H. Nature's Machinery, Repurposed: Expanding the Repertoire of Iron-Dependent Oxygenases. *ACS Catal.* **2020**, *10*, 12239−12255.

(21) Steck, V.; Kolev, J. N.; Ren, X.; Fasan, R. Mechanism-Guided Design and Discovery of Efficient Cytochrome P450-Derived C−H Amination Biocatalysts. *J. Am. Chem. Soc.* **2020**, *142*, 10343−10357.

(22) Roy, S.; Vargas, D. A.; Ma, P.; Sengupta, A.; Zhu, L.; Houk, K. N.; Fasan, R. Stereoselective construction of β-, γ- and δ-lactam rings via enzymatic C-H amidation. *Nat. Catal.* **2024**, *7*, 65−76.

(23) Prier, C. K.; Zhang, R. K.; Buller, A. R.; Brinkmann-Chen, S.; Arnold, F. H. Enantioselective, intermolecular benzylic C−H amination catalysed by an engineered iron-haem enzyme. *Nat. Chem.* **2017**, *9*, 629−634.

(24) Singh, R.; Kolev, J. N.; Sutera, P. A.; Fasan, R. Enzymatic C(sp^3)−H Amination: P450-Catalyzed Conversion of Carbonazidates into Oxazolidinones. *ACS Catal.* **2015**, *5*, 1685−1691.
(25) Cho, I.; Prier, C. K.; Jia, Z.-J.; Zhang, R. K.; Görbe, T.; Arnold, F. H. Enantioselective Aminohydroxylation of Styrenyl Olefins Catalyzed by an Engineered Hemoprotein. *Angew. Chem., Int. Ed.* **2019**, *58*, 3138−3142.
(26) Jia, Z.-J.; Gao, S.; Arnold, F. H. Enzymatic Primary Amination of Benzylic and Allylic C(sp^3)−H Bonds. *J. Am. Chem. Soc.* **2020**, *142*, 10279−10283.
(27) Liu, Z.; Qin, Z.-Y.; Zhu, L.; Athavale, S. V.; Sengupta, A.; Jia, Z.-J.; Garcia-Borràs, M.; Houk, K. N.; Arnold, F. H. An Enzymatic Platform for Primary Amination of 1-Aryl-2-alkyl Alkynes. *J. Am. Chem. Soc.* **2022**, *144*, 80−85.
(28) Athavale, S. V.; Gao, S.; Das, A.; Mallojjala, S. C.; Alfonzo, E.; Long, Y.; Hirschi, J. S.; Arnold, F. H. Enzymatic Nitrogen Insertion into Unactivated C−H Bonds. *J. Am. Chem. Soc.* **2022**, *144*, 19097−19105.
(29) Athavale, S. V.; Gao, S.; Liu, Z.; Mallojjala, S. C.; Hirschi, J. S.; Arnold, F. H. Biocatalytic, Intermolecular C−H Bond Functionalization for the Synthesis of Enantioenriched Amides. *Angew. Chem., Int. Ed.* **2021**, *60*, 24864−24869.
(30) Das, A.; Long, Y.; Maar, R. R.; Roberts, J. M.; Arnold, F. H. Expanding Biocatalysis for Organosilane Functionalization: Enantioselective Nitrene Transfer to Benzylic Si−C−H Bonds. *ACS Catal.* **2024**, *14*, 148−152.
(31) Tsutsumi, H.; Katsuyama, Y.; Izumikawa, M.; Takagi, M.; Fujie, M.; Satoh, N.; Shin-ya, K.; Ohnishi, Y. Unprecedented Cyclization Catalyzed by a Cytochrome P450 in Benzastatin Biosynthesis. *J. Am. Chem. Soc.* **2018**, *140*, 6631−6639.
(32) Tinzl, M.; Diedrich, J. V.; Mittl, P. R. E.; Clémancey, M.; Reiher, M.; Proppe, J.; Latour, J.-M.; Hilvert, D. Myoglobin-Catalyzed Azide Reduction Proceeds via an Anionic Metal Amide Intermediate. *J. Am. Chem. Soc.* **2024**, *146*, 1957−1966.
(33) Goswami, M.; Lyaskovskyy, V.; Domingos, S. R.; Buma, W. J.; Woutersen, S.; Troeppner, O.; Ivanović-Burmazović, I.; Lu, H.; Cui, X.; Zhang, X. P.; Reijerse, E. J.; DeBeer, S.; van Schooneveld, M. M.; Pfaff, F. F.; Ray, K.; de Bruin, B. Characterization of Porphyrin-Co(III)-'Nitrene Radical' Species Relevant in Catalytic Nitrene Transfer Reactions. *J. Am. Chem. Soc.* **2015**, *137*, 5468−5479.
(34) Das, A.; Maher, A. G.; Telser, J.; Powers, D. C. Observation of a Photogenerated Rh_2 Nitrenoid Intermediate in C−H Amination. *J. Am. Chem. Soc.* **2018**, *140*, 10412−10415.
(35) Van Trieste, G. P., III; Reid, K. A.; Hicks, M. H.; Das, A.; Figgins, M. T.; Bhuvanesh, N.; Ozarowski, A.; Telser, J.; Powers, D. C. Nitrene Photochemistry of Manganese N-Haloamides. *Angew. Chem., Int. Ed.* **2021**, *60*, 26647−26655.
(36) Hayashi, T.; Tinzl, M.; Mori, T.; Krengel, U.; Proppe, J.; Soetbeer, J.; Klose, D.; Jeschke, G.; Reiher, M.; Hilvert, D. Capture and characterization of a reactive haem-carbenoid complex in an artificial metalloenzyme. *Nat. Catal.* **2018**, *1*, 578−584.
(37) Lewis, R. D.; Garcia-Borràs, M.; Chalkley, M. J.; Buller, A. R.; Houk, K. N.; Kan, S. B. J.; Arnold, F. H. Catalytic iron-carbene intermediate revealed in a cytochrome *c* carbene transferase. *Proc. Natl. Acad. Sci. U. S. A.* **2018**, *115*, 7308−7313.
(38) Serrano-Plana, J.; Oloo, W. N.; Acosta-Rueda, L.; Meier, K. K.; Verdejo, B.; García-España, E.; Basallote, M. G.; Münck, E.; Que, L., Jr; Company, A.; Costas, M. Trapping a Highly Reactive Nonheme Iron Intermediate That Oxygenates Strong C−H Bonds with Stereoretention. *J. Am. Chem. Soc.* **2015**, *137*, 15833−15842.
(39) Zhang, J.; Hou, C.; Li, W.; Xu, H.; Zhao, C. Study on C−H amination reactions catalyzed by iron porphyrin nitrene complexes with different nitrogen sources. *Inorg. Chem. Commun.* **2020**, *114*, 107787.
(40) Chatterjee, S.; Harden, I.; Bistoni, G.; Castillo, R. G.; Chabbra, S.; van Gastel, M.; Schnegg, A.; Bill, E.; Birrell, J. A.; Morandi, B.; Neese, F.; DeBeer, S. A Combined Spectroscopic and Computational Study on the Mechanism of Iron-Catalyzed Aminofunctionalization of Olefins Using Hydroxylamine Derived N−O Reagent as the "Amino" Source and "Oxidant". *J. Am. Chem. Soc.* **2022**, *144*, 2637−2656.
(41) Mai, B. K.; Neris, N. M.; Yang, Y.; Liu, P. C−N Bond Forming Radical Rebound Is the Enantioselectivity-Determining Step in P411-Catalyzed Enantioselective C(sp^3)−H Amination: A Combined Computational and Experimental Investigation. *J. Am. Chem. Soc.* **2022**, *144*, 11215−11225.
(42) Gao, S.; Das, A.; Alfonzo, E.; Sicinski, K. M.; Rieger, D.; Arnold, F. H. Enzymatic Nitrogen Incorporation Using Hydroxylamine. *J. Am. Chem. Soc.* **2023**, *145*, 20196−20201.
(43) Rodríguez-López, J. N.; Lowe, D. J.; Hernández-Ruiz, J.; Hiner, A. N. P.; García-Cánovas, F.; Thorneley, R. N. F. Mechanism of Reaction of Hydrogen Peroxide with Horseradish Peroxidase: Identification of Intermediates in the Catalytic Cycle. *J. Am. Chem. Soc.* **2001**, *123*, 11838−11847.
(44) Makris, T. M.; Davydov, R.; Denisov, I. G.; Hoffman, B. M.; Sligar, S. G. MECHANISTIC ENZYMOLOGY OF OXYGEN ACTIVATION BY THE CYTOCHROMES P450. *Drug Metab. Rev.* **2002**, *34*, 691−708.
(45) Onderko, E. L.; Silakov, A.; Yosca, T. H.; Green, M. T. Characterization of a selenocysteine-ligated P450 compound I reveals direct link between electron donation and reactivity. *Nat. Chem.* **2017**, *9*, 623−628.
(46) Nash, K. M.; Rockenbauer, A.; Villamena, F. A. Reactive Nitrogen Species Reactivities with Nitrones: Theoretical and Experimental Studies. *Chem. Res. Toxicol.* **2012**, *25*, 1581−1597.
(47) Lee, W.-C. C.; Wang, J.; Zhu, Y.; Zhang, X. P. Asymmetric Radical Bicyclization for Stereoselective Construction of Tricyclic Chromanones and Chromanes with Fused Cyclopropanes. *J. Am. Chem. Soc.* **2023**, *145*, 11622−11632.
(48) Li, F.; Xiao, L.; Liu, L. Metal-Diazo Radicals of α-Carbonyl Diazomethanes. *Sci. Rep.* **2016**, *6*, 22876.
(49) McDonald, C. C.; Phillips, W. D.; Mower, H. F. An electron spin resonance study of some complexes of iron, nitric oxide, and anionic ligands. *J. Am. Chem. Soc.* **1965**, *87*, 3319−3326.
(50) Kon, H. Paramagnetic resonance study of nitric oxide hemoglobin. *J. Biol. Chem.* **1968**, *243*, 4350−4357.
(51) Yonetani, T.; Yamamoto, H.; Erman, J. E.; Leigh, J. S., Jr; Reed, G. H. Electromagenetic properties of hemoproteins. V. Optical and electron paramagnetic resonance characteristics of nitric oxide derivatives of metalloporphyrin-apohemoprotein complexes. *J. Biol. Chem.* **1972**, *247*, 2447−2455.
(52) Brunori, M.; Falcioni, G.; Rotilio, G. Kinetic properties and electron paramagnetic resonance spectra of the nitric oxide derivative of hemoglobin components of trout (*Salmo irideus*). *Proc. Natl. Acad. Sci. U. S. A.* **1974**, *71*, 2470−2472.
(53) Deatherage, J. F.; Moffat, K. Structure of nitric oxide hemoglobin. *J. Mol. Biol.* **1979**, *134*, 401−417.
(54) Sancier, K. M.; Freeman, G.; Mills, J. S. Electron spin resonance of nitric oxide-hemoglobin complexes in solution. *Science* **1962**, *137*, 752−754.
(55) Hori, H.; Ikeda-Saito, M.; Yonetani, T. Electromagnetic properties of hemoproteins. VI. Single crystal EPR of myoglobin nitroxide. Freezing-induced reversible changes in the molecular orientation of the ligand. *J. Biol. Chem.* **1981**, *256*, 7849−7855.
(56) Woolum, J. C.; Tiezzi, E.; Commoner, B. Electron spin resonance of iron-nitric oxide complexes with amino acids, peptides and proteins. *Biochim. Biophys. Acta, Protein Struct.* **1968**, *160*, 311−320.
(57) Smith, M. A.; Majer, S. H.; Vilbert, A. C.; Lancaster, K. M. Controlling a burn: outer-sphere gating of hydroxylamine oxidation by a distal base in cytochrome P460. *Chem. Sci.* **2019**, *10*, 3756−3764.
(58) Coleman, R. E.; Lancaster, K. M. Heme P460: A (Cross) Link to Nitric Oxide. *Acc. Chem. Res.* **2020**, *53*, 2925−2935.
(59) Bollmeyer, M. M.; Majer, S. H.; Coleman, R. E.; Lancaster, K. M. Outer coordination sphere influences on cofactor maturation and substrate oxidation by cytochrome P460. *Chem. Sci.* **2023**, *14*, 8295−8304.

https://doi.org/10.1021/jacs.4c05761
J. Am. Chem. Soc. 2024, 146, 20556−20562

(60) Doctorovich, F.; Bikiel, D.; Pellegrino, J.; Suárez, S. A.; Larsen, A.; Martí, M. A. Nitroxyl (azanone) trapping by metalloporphyrins. *Coord. Chem. Rev.* **2011**, *255*, 2764−2784.
(61) Reisz, J. A.; Bechtold, E.; King, S. B. Oxidative heme protein-mediated nitroxyl (HNO) generation. *Dalton Trans.* **2010**, *39*, 5203−5212.
(62) Ascenzi, P.; De Simone, G.; Ciaccio, C.; Santucci, R.; Coletta, M. Hydroxylamine-induced oxidation of ferrous CO-bound carboxymethylated-cytochrome *c*. *J. Porphyrins Phthalocyanines* **2018**, *22*, 1082−1091.
(63) Kuznetsova, S.; Knaff, D. B.; Hirasawa, M.; Sétif, P.; Mattioli, T. A. Reactions of Spinach Nitrite Reductase with Its Substrate, Nitrite, and a Putative Intermediate, Hydroxylamine. *Biochemistry* **2004**, *43*, 10765−10774.
(64) Einsle, O.; Messerschmidt, A.; Stach, P.; Bourenkov, G. P.; Bartunik, H. D.; Huber, R.; Kroneck, P. M. H. Structure of cytochrome *c* nitrite reductase. *Nature* **1999**, *400*, 476−480.
(65) Kroneck, P. M. H. Nature's nitrite-to-ammonia expressway, with no stop at dinitrogen. *J. Biol. Inorg. Chem.* **2022**, *27*, 1−21.
(66) Miranda, K. M.; Nims, R. W.; Thomas, D. D.; Espey, M. G.; Citrin, D.; Bartberger, M. D.; Paolocci, N.; Fukuto, J. M.; Feelisch, M.; Wink, D. A. Comparison of the reactivity of nitric oxide and nitroxyl with heme proteins: A chemical discussion of the differential biological effects of these redox related products of NOS. *J. Inorg. Biochem.* **2003**, *93*, 52−60.
(67) For a detailed discussion on the EPR features of the $S = 1/2$ intermediate being similar to that of a six-coordinate $\{FeNO\}^7$, refer to Section 5 of the Supporting Information.
(68) Bari, S. E.; Amorebieta, V. T.; Gutiérrez, M. M.; Olabe, J. A.; Doctorovich, F. Disproportionation of hydroxylamine by water-soluble iron(III) porphyrinate compounds. *J. Inorg. Biochem.* **2010**, *104*, 30−36.
(69) McQuarters, A. B.; Goodrich, L. E.; Goodrich, C. M.; Lehnert, N. Disproportionation of *O*-Benzylhydroxylamine Catalyzed by a Ferric Bis-Picket Fence Porphyrin Complex. *Z. Anorg. Allg. Chem.* **2013**, *639* (8−9), 1520−1526.
(70) Einsle, O.; Messerschmidt, A.; Huber, R.; Kroneck, P. M. H.; Neese, F. Mechanism of the Six-Electron Reduction of Nitrite to Ammonia by Cytochrome *c* Nitrite Reductase. *J. Am. Chem. Soc.* **2002**, *124*, 11737−11745.
(71) Bykov, D.; Neese, F. Six-electron reduction of nitrite to ammonia by cytochrome *c* nitrite reductase: insights from density functional theory studies. *Inorg. Chem.* **2015**, *54*, 9303−9316.

https://doi.org/10.1021/jacs.4c05761
J. Am. Chem. Soc. 2024, 146, 20556−20562